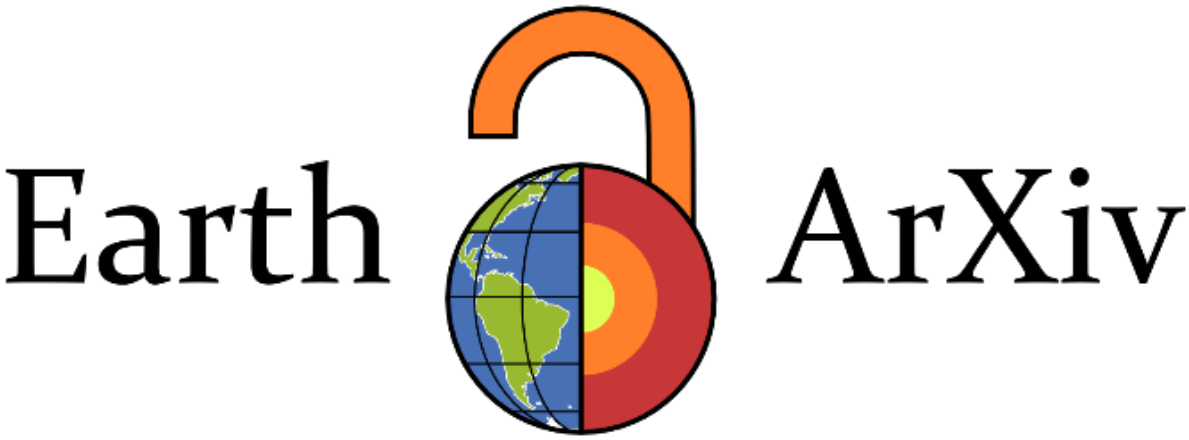

Differential Impacts of Marine Heatwaves and Coldwaves on Air-Sea CO_2 Flux Across Global Oceans

Zhao Meng[a]

[a]Tsinghua Shenzhen International Graduate School, Tsinghua University, Shenzhen 518052, China

Abstract

The contrasting impacts of marine heatwaves (MHWs) and marine cold waves (MCWs) on the ocean carbon cycle remain insufficiently understood. Based on observational and reanalysis data from 1990 to 2019, this study investigates the global-scale responses of air-sea CO2 fluxes (FCO2) to MHWs and MCWs. Results reveal that MHWs and MCWs exert opposing influences on FCO2, with the magnitude of MCW-induced changes approximately three times greater than those associated with MHWs. These responses exhibit pronounced spatial heterogeneity. Notably, the North Pacific subpolar region, Arabian Sea, equatorial central Pacific, and Southern Ocean subpolar region display patterns that deviate from global tendencies. Among them, the equatorial central Pacific emerges as a key driver of interannual variability in both global FCO2 and surface ocean partial pressure of CO2 (pCO2sea). In the Arabian Sea, FCO2 variability is primarily modulated by wind speed, whereas in the other three regions, pCO2sea plays a dominant role. While temperature variations largely control pCO2sea in most areas, non-thermal processes dominate in the four anomalous regions. In particular, freshwater fluxes from precipitation and evaporation, together with equatorial upwelling, are identified as critical regulators of FCO2 in the equatorial central Pacific. These findings advance our understanding of how extreme thermal events shape the ocean carbon sink and provide a scientific basis for improved carbon cycle assessments under ongoing climate change.

Key Words:

Marine heatwaves, marine coldwaves, air-sea CO_2 fluxes, global ocean

1、Introduction

Global climate warming is profoundly altering Earth's climate system, exerting extensive and far-reaching impacts on the marine environment (Collins et al., 2010; Boer et al., 2011; Frölicher et al., 2018; Alizadeh, 2024). In recent decades, marine heatwaves (MHWs) and marine cold waves (MCWs), as extreme temperature events, have exhibited notable changes in their frequency, intensity, duration, and spatial distribution (Frölicher et al., 2018; Laufkötter et al., 2020). Observations indicate a significant increase in the occurrence of MHWs, contributing to anomalous sea surface temperatures (SST) rises across multiple ocean basins. In contrast, while MCWs are becoming less frequent and intense, their ecological impacts remain substantial, driving disruptions in ecosystem structure and function (Frölicher et al., 2018; Hobday et al., 2016; 2018; Smale et al., 2019; Oliver et al., 2021; Chiswell S M, 2022; Yao Y, et al.,2022; Meque et al., 2024; Quesada et al., 2023; Deser et al., 2024). MHWs and MCWs arise from multi-scale ocean-atmosphere interactions, including anomalous air-sea heat fluxes, variations in horizontal and vertical heat transport, and dynamic processes such as wind anomalous and upwelling changes (Ratnam et al., 2016; Holbrook et al., 2019; Mandal et al., 2023; Athira et al., 2024). On interannual to decadal scales, these events are closely linked to large-scale climate modes such as the El Niño-Southern Oscillation (ENSO), which modulates their spatial and temporal characteristics (Smale et al., 2019; Oliver et al., 2021). These extreme temperature events directly influence the thermal state of the ocean, thereby having profound effects on marine ecosystems and biodiversity, including alterations in species distribution, reshaping of community structure, and impacts on fishery resources (Frölicher and Laufkötter, 2018; Smale et al., 2019; Cheung et al., 2021; Schlegel et al., 2021; Smith et al., 2021; Guo et al., 2022).

The primary driver of global climate warming is carbon dioxide (CO2) (IPCC, 2021). Concurrently, the oceans serve as the largest active carbon reservoir in the Earth system, absorbing approximately 25% of anthropogenic CO2 emissions annually. This process plays a critical role in mitigating the rise of atmospheric CO2

concentrations and regulating the global carbon cycle and climate system (DeVries et al., 2019; DeVries et al., 2023; Friedlingstein et al., 2024; Resplandy et al., 2024). The air-sea CO2 flux (FCO2) is a key indicator of the ocean's carbon sink capacity, exhibiting significant regional heterogeneity in its spatiotemporal distribution (Iida et al., 2015; Sarma et al., 2023; Fay et al., 2024). Variability in FCO2 is primarily influenced by a combination of physical and biogeochemical processes in the ocean, including ocean circulation patterns, phytoplankton primary productivity, the balance of the seawater carbonate system, and the dynamics of air-sea exchange (Joos et al., 1999; Gattuso et al., 2015; Edwing et al., 2024; Yang et al., 2024; Li et al., 2024). Furthermore, extreme temperature events can significantly affect local and even global FCO2 distributions by altering surface seawater temperature, wind stress, nutrient supply, and dissolved inorganic carbon concentrations (Johnson et al., 2021). Therefore, systematically studying the impacts of marine heatwaves (MHWs) and marine cold waves (MCWs) on air-sea CO_2 exchange is essential for a deeper understanding of the dynamic regulatory mechanisms of the ocean carbon cycle and its feedback effects on the climate system.

In recent years, significant advancements have been made in understanding the impacts and mechanisms of extreme temperature events on regional seawater CO2 partial pressure (pCO_2) and air-sea CO_2 flux (FCO_2), driven by improvements in observational technologies and numerical simulations. Research indicates that responses to extreme temperature events exhibit considerable regional heterogeneity across different marine areas (Yang et al., 2024; Li et al., 2024). For instance, Mignot et al. (2022) found that intense and prolonged marine heatwaves (MHWs) significantly suppressed CO2 release in the equatorial Pacific by altering the strength of upwelling in that region, while also diminishing the CO2 absorption capacity of the mid-latitude North Pacific (Mignot et al., 2022). Furthermore, Duke et al. (2023) highlighted that during MHWs, the weakening of winter vertical mixing in the subpolar North Pacific circulation inhibited the upwelling of deep, carbon-rich water, leading to an anomalous increase in CO_2 absorption (Duke et al., 2023). Additionally, Li et al. (2024) conducted a comprehensive assessment of the regional impacts of

MHWs on air-sea CO_2 exchange across different global marine areas, utilizing multi-source data integration and modeling, thereby providing new insights into the spatial heterogeneity of extreme temperature events (Li et al., 2024).

Despite significant progress in related research in recent years, several critical scientific questions remain to be thoroughly explored. First, although some studies have focused on the impact of Marine Heat Waves (MHWs) on global air-sea CO2 flux (FCO2), the driving mechanisms behind their anomalous variations are still not systematically understood. Second, research on the effects of Marine Cold Waves (MCWs) on the global ocean carbon cycle is relatively sparse, and the differences between MHWs and MCWs in regulating FCO2 have not been adequately investigated. These research gaps limit our understanding of how extreme temperature events modulate the ocean's carbon sink function throughout the year. To address these gaps, this study utilizes observational and reanalysis data from 1990 to 2019 to quantitatively assess the differential regulatory roles of MHWs and MCWs on global air-sea FCO2, revealing their spatial and temporal variability and exploring the potential driving mechanisms behind significant anomalies in FCO2. The structure of this paper is as follows: Section 2 presents the data sources and analytical methods; Section 3 analyzes the spatial and temporal variations of global FCO2 and sea surface partial pressure of CO2 (pCO2sea) under the influence of MHWs and MCWs; Section 4 discusses the regulatory role of the equatorial central Pacific region (notable for significant FCO2 anomalies) on interannual variations of global FCO2 and pCO2sea, as well as the potential dynamic mechanisms of extreme temperature events in this region; Section 5 summarizes the main findings and suggests directions for future research.

2、Data and Methods

2.1 Data

This study investigates the surface partial pressure of CO2 (pCO2sea), CO2 flux (FCO2), sea surface temperature (SST), sea surface salinity (SSS), wind speed (U10),

dissolved inorganic carbon (DIC), and precipitation using multiple datasets. The details of the datasets are as follows:

The SST data utilized in this research is derived from the daily Optimal Interpolation Sea Surface Temperature (OISST) v2.1 dataset published by the National Oceanic and Atmospheric Administration (NOAA) (Huang et al., 2021). This dataset is based on global observational data and offers high spatiotemporal resolution. To assess anomalies in CO2 flux during marine heatwaves (MHWs), we employed the SeaFlux version 2021.04 observational dataset product (Fay et al., 2021). This product integrates six internationally recognized datasets for FCO2 and pCO2sea (Chau et al., 2022; Denvil-Sommer et al., 2019; Gregor et al., 2019; Iida et al., 2020; Landschützer et al., 2014, 2020; Rödenbeck et al., 2013; Zeng et al., 2014), all of which are developed based on the Surface Ocean CO2 Atlas (SOCAT, Bakker et al., 2016), ensuring data accuracy and consistency.

Moreover, this study incorporates auxiliary data from multiple sources to comprehensively analyze the ocean-atmosphere interaction processes. Sea surface salinity data is sourced from the Simple Ocean Data Assimilation (SODA) ocean reanalysis dataset. Wind field, precipitation rate, and evaporation rate data are obtained from the ERA5 (ECMWF Reanalysis 5th Generation) reanalysis product developed by the European Centre for Medium-Range Weather Forecasts (ECMWF). DIC and total alkalinity (TA) data are derived from the Japan Meteorological Agency (JMA) dataset. The three-dimensional ocean circulation fields, including zonal, meridional, and vertical flows, are obtained from the Global Ocean Data Assimilation System (GODAS) provided by the National Centers for Environmental Prediction (NCEP). The comprehensive application of these high-quality datasets provides a reliable foundation for in-depth research on air-sea exchange processes during marine heatwaves.

2.2 Estimation and decomposition of FCO_2 and pCO_{2sea}

In the analysis of five observationally-based products and biogeochemical

datasets, the sea-air CO2 flux density (FCO2) was calculated using surface seawater CO2 partial pressure (pCO2sea) data and a gas exchange formula:

$$F_{CO2} = k a(pCO_{2sea} - pCO_{2air})$$

Where “a” represents the solubility of CO2 in seawater,”k” is the gas exchange coefficient, “pCO_{2air}” is the atmospheric CO2 partial pressure, and “pCO_{2sea}” is the surface seawater CO2 partial pressure. In this equation, a negative value of FCO2 indicates that the ocean is absorbing CO2 from the atmosphere, while a positive value indicates that the ocean is releasing CO2 into the atmosphere.

To determine the driving mechanisms behind the anomalies in FCO2 during global Marine Heat Waves (MHW) and Marine Cold Waves (MCW), we conducted a first-order Taylor series expansion of the FCO2 anomalies:

$$F_{CO2}{}' = (ka)'(\overline{pCO_{2sea} - pCO_{2air}}) + \overline{(ka)}pCO_{2sea}{}' - \overline{(ka)}pCO_{2air}{}'$$

The terms on the right side represent the contributions to $F_{CO2}{}'$: the first term reflects the anomalous effects of gas exchange rates and solubility. It is important to note that the temperature dependence of “k” and “a” can offset each other, thus $(ka)'$ primarily driven by variations in wind speed. The second term accounts for the anomalous effects of surface seawater CO_2 partial pressure, while the third term represents the anomalous effects of atmospheric CO_2 partial pressure.

Additionally, we decomposed the anomalies in pCO_{2sea} to analyze the impacts of temperature and non-temperature factors on these anomalies.

$$npCO_{2t}{}' = \overline{pCO_{2sea}} \times \exp(0.0423 \times (SST - \overline{SST})) - \overline{pCO_{2sea}}$$

$$npCO_{2nt}{}' = pCO_{2sea} \times \exp(0.0423 \times (\overline{SST} - SST)) - \overline{pCO_{2sea}}$$

We further separated pCO2sea into contributions from sea surface temperature (SST), dissolved inorganic carbon (DIC), total alkalinity (TA), and sea surface salinity (SSS) to discuss which factors influenced the global pCO_{2sea} anomaly variations during MHW and MCW.

$$dpCO_{2sea} = \frac{\partial pCO_{2sea}}{\partial T} dT + \frac{\partial pCO_{2sea}}{\partial DIC} dDIC + \frac{\partial pCO_{2sea}}{\partial ALK} dALK + \frac{\partial pCO_{2sea}}{\partial S} dS$$

In this context, dpCO2sea denotes the changes in surface seawater CO2 partial pressure (pCO2sea), while T、 ALK, and S represent sea surface temperature (SST), total alkalinity (TA), and sea surface salinity (SSS), respectively.

2.3 MHW and MCW diagnostic methods

According to the definition by Hobday et al. (2016), marine heatwaves (MHW) are defined as anomalous warming events where sea surface temperatures (SST) exceed the 90th percentile and persist for five days or longer. Conversely, marine coldwaves (MCW) are characterized by SSTs falling below the 10th percentile for the same duration. To account for the potential influence of seasonal temperature variations, we calculated daily SST anomalies by removing the seasonal cycle, specifically by subtracting the long-term climatic average SST for each day. This approach allows the thresholds to vary seasonally, enabling the detection of MHWs in summer and warm events in winter, which is critical for investigating the potential ecological impacts across different seasons. Furthermore, we utilized daily temperature data from all years, along with data from an 11-day window centered on each day, to compute the climatic thresholds and averages for each day of the year. Subsequently, we applied a 31-day moving window for smoothing to eliminate short-term noise and fluctuations, resulting in more stable and reliable data.

Given that the existing FCO_2 and pCO_{2sea} inversion data only include monthly data from 1990 to 2019, we defined months with more than 15 days of MHW or MCW as MHW months or MCW months, respectively. This study focuses on these MHW and MCW months, as they experienced significant MHW and MCW events.

2.4 Random Forest and Permutation Testing

To elucidate the key dynamic mechanisms influencing the anomalous variations in air-sea CO_2 flux (FCO_2) and sea surface partial pressure of CO_2 (pCO_{2sea}) during marine heatwave (MHW) and marine cold wave (MCW) events in the central equatorial Pacific, this study employed a machine learning-based Random Forest

Regression model. A systematic modeling analysis was conducted to assess the anomalous changes in various environmental factors. By constructing a multivariable regression model, we quantified the contributions of different environmental factors, such as sea surface temperature, salinity, wind field, three-dimensional circulation, precipitation, and evaporation, to the anomalies in FCO_2 and pCO_{2sea}. To further identify the dominant factors, we utilized feature importance assessment methods, including Feature Importance Analysis and Permutation Testing, to quantitatively evaluate the significance of the input variables in the model. This allowed us to identify the key dynamic factors that significantly influence the anomalous changes in FCO_2 and pCO_{2sea}. This approach not only effectively captures nonlinear relationships but also provides new insights into the complex interactions between the ocean and atmosphere.

3、Results

3.1、Global Changes in Ocean Carbon Sink Induced by MHW and MCW

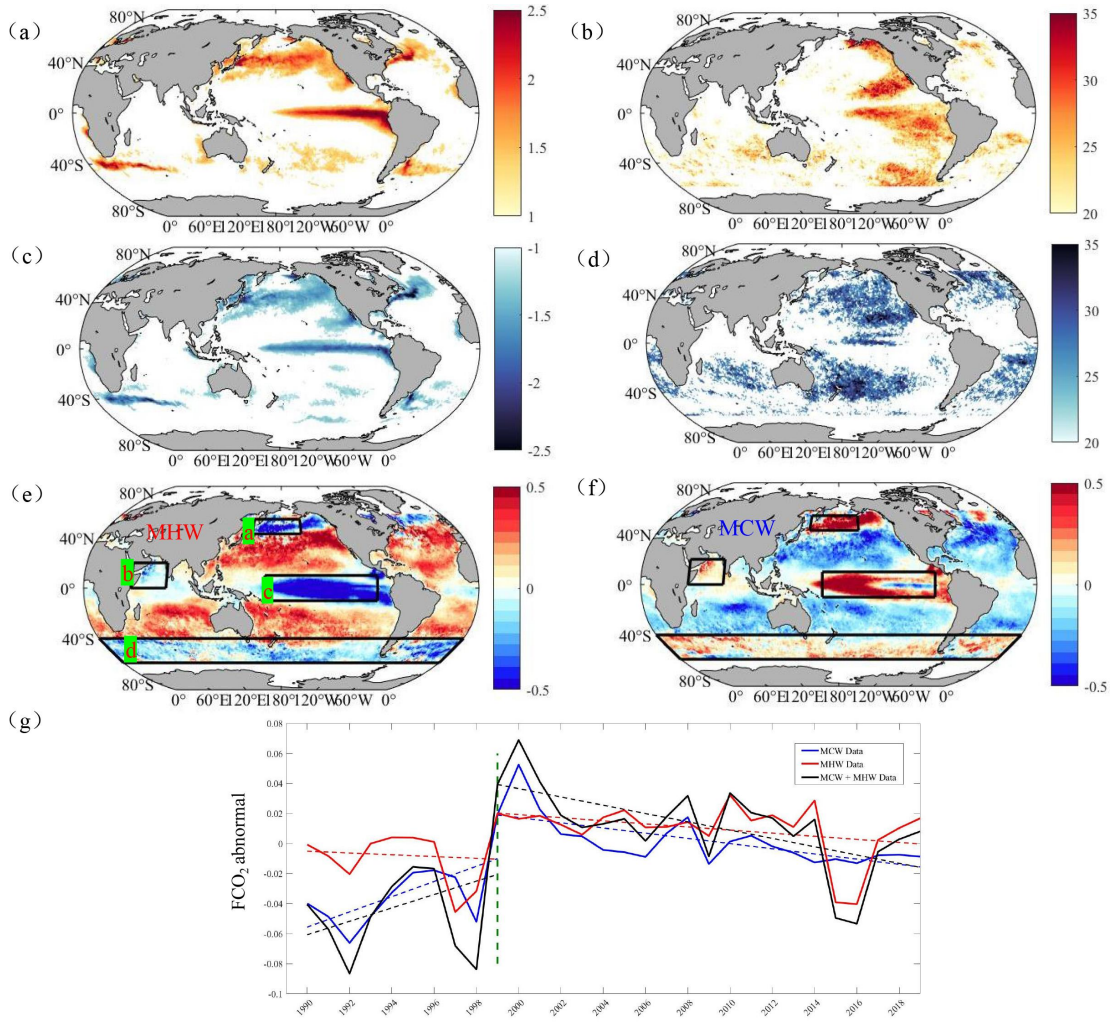

Figure 1. The amplitude (a,c) and occurrence frequency (b,d) of marine heatwave (MHW) (a,b) and marine coldwave (MCW) (c,d) events for each grid point from 1990 to 2019. Spatial distribution (e,f) and interannual changes (g) of FCO_2 abnormal caused by MHW and MCW. Figures a-d illustrate the data representing the first quartile. In figure (g), the detected change points are marked by vertical green dashed lines, while anomalous FCO_2 trends associated with extreme temperature events are depicted by slanted dashed lines in three distinct colors: blue for MCW, red for MHW, and black for the combined effects of total extreme temperature events.

Between 1990 and 2022, the global ocean (0-360° , -60° to 60°) experienced an increase of approximately 0.112 Pg in CO2 emissions during marine heatwave (MHW) events, while carbon absorption increased by about 0.312 Pg during marine cold spells (MCW). This impact exhibited significant spatial variability. As illustrated in Figure 1, FCO2 in the Southern Ocean south of 40° S, the equatorial Pacific, and certain regions north of 40° N decreased during MHW events but increased during

MCW, demonstrating a pattern that contrasts with the global trend. Notably, the changes in FCO2 were particularly pronounced in the subpolar North Pacific (Region a), the Arabian Sea (Region b), the equatorial central Pacific (Region c), and the subpolar Southern Ocean (Region d). Further quantification of FCO2 changes in these four critical regions revealed that the anomalous responses were most prominent in the northern North Pacific and the central Pacific.

From an interannual perspective, the global ocean's FCO_2 response to extreme temperature events has undergone a significant transformation, shifting from strong carbon absorption in earlier years to a trend of weak emissions. An analysis of FCO2 anomalies from 1990 to 2019 identified 1999 as a critical turning point. Prior to this year, MHWs enhanced the ocean's capacity to absorb CO_2, resulting in negative FCO_2 changes, while MCWs led to positive increases in FCO2, indicating a gradual weakening of the ocean carbon sink. During this period, the anomalous FCO2 changes driven by extreme temperature events were predominantly influenced by MCWs. Since 1999, however, there has been a notable shift in the FCO2 response to extreme temperature events, with MHWs becoming increasingly important as a driving factor. Specifically, MHWs typically resulted in positive FCO2 values, enhancing the ocean's release of CO2 to the atmosphere, while MCWs also exhibited characteristics that promoted CO_2 release in certain years. Compared to the period before 1999, the facilitative effect of MHWs on CO2 emissions has significantly intensified, while the capacity of MCWs to mitigate ocean CO_2 release has markedly diminished. This transition may be closely linked to changes in oceanic physical and biogeochemical processes under the backdrop of global warming.

Statistical analysis further confirms the shift in the dominant pattern of FCO2 associated with extreme temperature events. Prior to 1999, the correlation coefficient between FCO2 anomalies induced by marine cold waves (MCWs) and total FCO2 anomalies was $r = 0.89$ ($p < 0.05$). During marine heatwaves (MHWs), this correlation coefficient was $r = 0.83$ ($p < 0.05$). After 1999, the correlation during MHWs decreased to $r = 0.76$ ($p < 0.05$), while the correlation during MCWs remained relatively high at $r = 0.83$ ($p < 0.05$). This shift may have been influenced by specific

extreme temperature events in certain years. For instance, the MCW event in 2000 resulted in positive global ocean FCO2 anomalies, whereas the MHW events of 1997-1998 and 2015-2016 significantly enhanced the ocean's capacity to absorb CO2. These key events may have accelerated the process of changing the dominant pattern.

Furthermore, it is noteworthy that, theoretically, global warming should amplify the promoting effect of MHWs on oceanic CO_2 emissions while diminishing the enhancing effect of MCWs on oceanic CO2 absorption. However, observational data indicate that since 1999, MHWs, MCWs, and overall extreme temperature events have shown a negative enhancement trend, collectively increasing the ocean's carbon sink capacity. This seemingly paradoxical phenomenon may arise from the synergistic effects of multiple mechanisms, and future research should further investigate its underlying drivers.

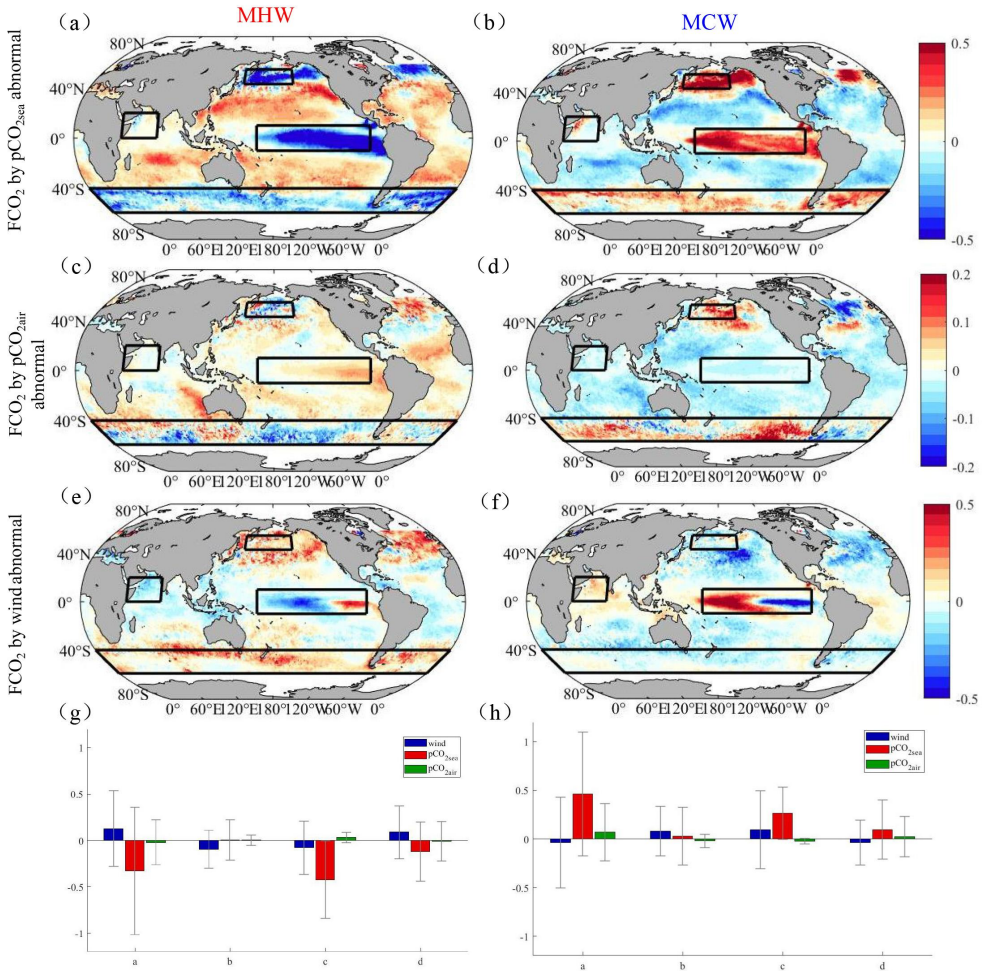

Figure 2. Spatial distribution of FCO_2 anomalies and they driven by wind (a,b), pCO_{2sea}(c,d), and pCO_{2air} (e,f), during MHW and MCW periods.

Through a first-order Taylor expansion of FCO2 anomalies during Marine Heat Waves (MHW) and Marine Cold Waves (MCW), we found that the spatial distribution of FCO2 changes driven by pCO2sea closely resembles that of total FCO2 changes, indicating that pCO2sea is the primary driver of FCO2 anomalies. In contrast, changes in FCO2 driven by pCO2air were relatively minor; during MHW, variations in pCO2air in regions a and d resulted in increased FCO2, while other regions exhibited a decreasing trend. During MCW, the pattern was reversed. Changes in FCO2 due to wind fields displayed significant spatial variability: during MHW, FCO2 increased in high-latitude regions and decreased in low-latitude regions, while the opposite trend was observed during MCW. Notably, in the central Pacific (region c), wind field changes in the eastern area during MHW led to an increase in FCO2, whereas in the western area, the wind field changes resulted in a decrease in FCO2. Conversely, during MCW, wind field changes in the eastern area caused a decrease in FCO2, while those in the western area resulted in an increase. These results suggest that during both MHW and MCW, pCO2sea has the most significant impact on FCO2 anomalies, followed by wind fields, while the influence of pCO2air is relatively minor. Additionally, the effects of different driving factors exhibit notable spatial variability across different regions.

To further quantify the contributions of wind speed, pCO2 in the air, and pCO2 in the sea to the anomalies in FCO2 during Marine Heat Wave (MHW) and Marine Cold Wave (MCW) events, the results indicate the following: In the northern North Pacific (region a), the average CO2 absorption increased by 0.206 mol m^{-2} yr^{-1} ($p < 0.05$) during MHW, primarily driven by changes in pCO2sea. Conversely, during MCW, the average CO2 absorption decreased by 0.214 mol m^{-2} yr^{-1} ($p< 0.05$), also predominantly influenced by anomalies in pCO2sea. In the Arabian Sea (region b), CO2 absorption increased on average by 0.075 mol m^{-2} yr^{-1} ($p < 0.05$) during MHW, mainly driven by changes in wind speed; during MCW, CO2 absorption decreased by an average of 0.069 mol m^{-2} yr^{-1} ($p < 0.05$), similarly dominated by wind speed anomalies. In the central Pacific (region c), CO2 absorption increased by an average of 0.242 mol m^{-2} yr^{-1} ($p < 0.05$) during MHW, primarily driven by changes in

pCO2sea; during MCW, there was an average decrease of 0.112 mol m^{-2} yr^{-1} ($p < 0.05$), also predominantly influenced by pCO2sea anomalies. In the Southern Ocean (region d), CO2 absorption increased on average by 0.059 mol m^{-2} yr^{-1} ($p < 0.05$) during MHW, driven mainly by changes in pCO_{2sea}; during MCW, CO_2 absorption decreased by an average of 0.062 mol m^{-2} yr^{-1} ($p < 0.05$), again primarily influenced by anomalies in pCO_{2sea}.

3.2、Global pCO_{2sea} changes caused by MHW and MCW

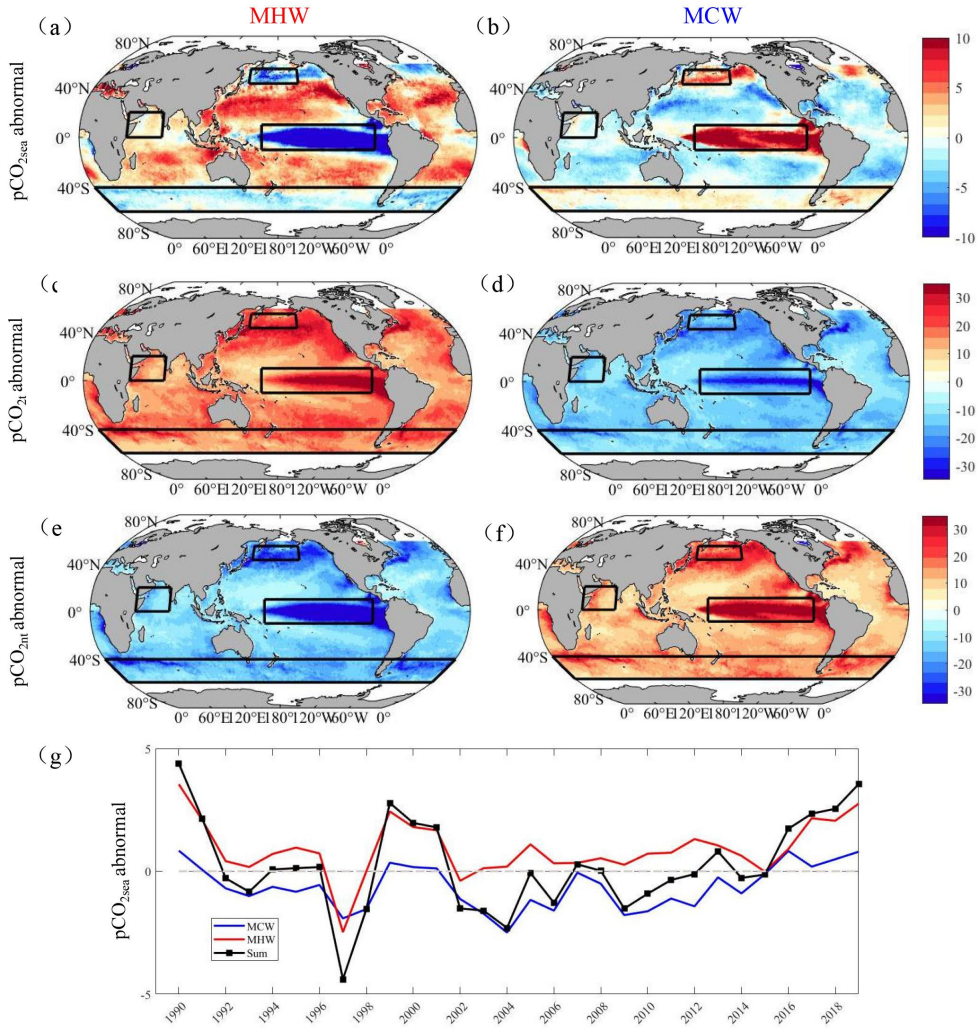

Figure 3. Changes in pCO_{2sea} anomalies (a,b) and the pCO_{2sea} anomalies driven by temperature (c,d) and non-temperature factors (e,f) across different regions and and interannual changes (g) of pCO_{2sea} abnormal during MHW and MCW periods.

We further analyzed the anomalies in sea surface partial pressure of carbon dioxide (pCO2sea) during marine heatwaves (MHWs) and marine cold spells (MCWs)

on a global scale. The results indicate a general increasing trend in pCO2sea during MHWs, while a decreasing trend is observed during MCWs. Furthermore, significant regional differences in pCO2sea variations were identified, particularly in the northern North Pacific (Region A), the central Pacific (Region C), and the Southern Ocean (Region D), where the anomalies in pCO2sea differ markedly from those in other regions. Specifically, MHW events typically lead to a reduction in pCO2sea anomalies in these regions, whereas other areas generally exhibit an increase in pCO2sea anomalies. In contrast, MCW events result in an increase in pCO2sea anomalies in Regions A and C, while other regions predominantly show a decrease. In Region A, the average pCO2sea decreased by 3.461 μatm during MHWs and increased by 4.141 μatm during MCWs. In Region B, the average pCO2sea increased by 1.188 μatm during MHWs and decreased by 0.390 μatm during MCWs. In Region C, the average pCO2sea decreased by 16.428 μatm during MHWs and increased by 7.917 μatm during MCWs. In Region E, the average pCO2sea decreased by 1.201 μatm during MHWs and increased by 0.948 μatm during MCWs.

Globally, during marine heatwave (MHW) events, the anomalies in sea surface partial pressure of carbon dioxide (pCO2sea) driven by temperature exhibit a general increasing trend, whereas anomalies induced by non-temperature factors show a decreasing trend. Conversely, during marine coldwave (MCW) events, these patterns are reversed. In the northern North Pacific (Region A), the central Pacific (Region C), and the Southern Ocean (Region D), pCO2sea variations during MHW and MCW periods are predominantly influenced by non-temperature factors, particularly in the central Pacific where the influence of non-temperature factors is especially pronounced. In contrast, in other marine regions, pCO2sea changes are primarily driven by temperature factors.

On an interannual scale, pCO2sea variations caused by extreme temperature events exhibit significant fluctuations. Overall, MHW events typically lead to an increase in global pCO2sea anomalies, while MCW events result in a decrease in these anomalies. However, in recent years, the global pCO2sea anomalies associated with MCW events have shifted from decreasing to increasing, while those related to

MHW events have intensified further. Notably, in 1997, both MHW and MCW events resulted in a significant decrease in pCO2sea, a phenomenon that warrants further investigation.

4、Discussion

4.1 、 The role of the equatorial Central Pacific Ocean in regulating the interannual variation of FCO2 and pCO2sea during the global MHW and MCW

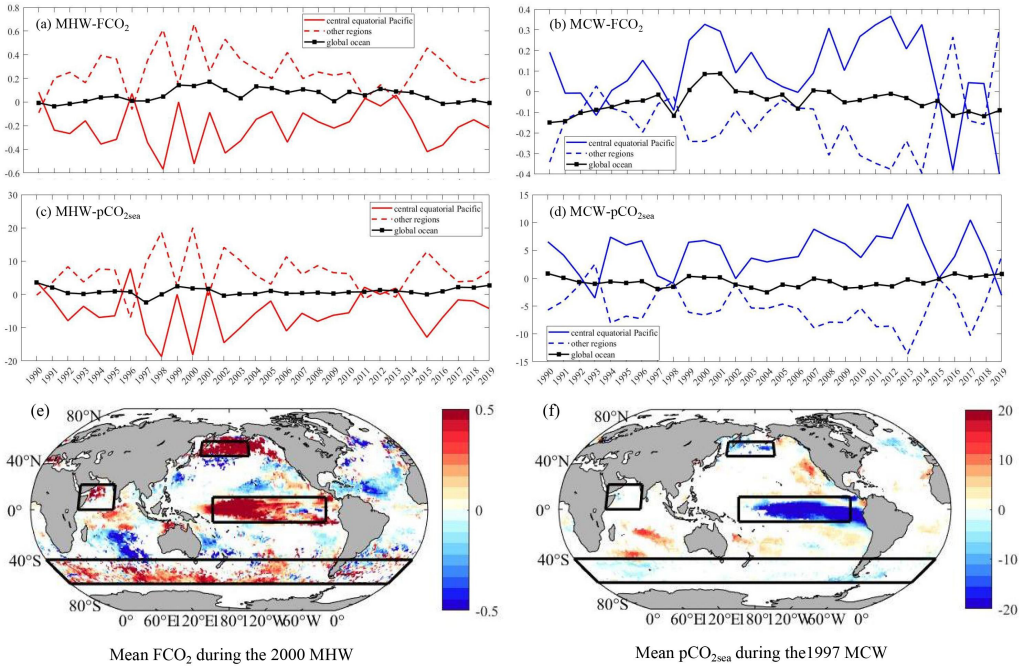

Figure 4. Interannual variability of FCO_2 and pCO_{2sea} anomalies in the central equatorial Pacific and other oceanic regions during MHWs and MCWs. Interannual variability of FCO_2 induced by MHWs and MCWs (a, b), interannual variability of pCO_{2sea} induced by MHWs and MCWs (c, d), spatial distribution of global FCO_2 anomalies during the 2000 MCW event (e), and spatial distribution of global pCO_{2sea} anomalies during the 1997 MHW event. The smooth solid line represents the central equatorial Pacific, the smooth dashed line represents other oceanic regions outside the central equatorial Pacific, the solid line with nodes represents global oceanic regions, the red line denotes changes induced by MHWs, and the blue line indicates changes induced by MCWs.

We conducted a focused analysis of the role of the equatorial central Pacific in the interannual anomalies of FCO2 and pCO2sea during global marine heatwave (MHW) and marine cold wave (MCW) events, with the aim of determining whether it significantly regulates the interannual trends of global FCO2 and pCO2sea anomalies.

Our findings reveal that during MHW and MCW events, the interannual anomalies of FCO2 and pCO2sea in the equatorial central Pacific exhibit markedly opposite characteristics compared to other oceanic regions (see Figures 4a-d). Specifically, during MHW, there is a general enhancement in CO2 absorption in the equatorial central Pacific; however, the statistical correlation between FCO2 anomalies in this region and global FCO2 anomalies is not significant ($p > 0.05$). In contrast, pCO2sea anomalies show a general decrease and are significantly positively correlated with global pCO_{2sea} anomalies ($r = 0.51$, $p < 0.05$). Conversely, during MCW, CO_2 absorption in the equatorial central Pacific weakens, and the FCO_2 anomalies exhibit a significant positive correlation with global FCO2 anomalies ($r = 0.58$, $p < 0.05$), while the increase in pCO_{2sea} anomalies shows no significant correlation with global pCO_{2sea} changes ($p > 0.05$). Notably, in recent years during MCW, the FCO_2 anomalies in the equatorial central Pacific have demonstrated a trend of enhanced CO2 absorption, potentially linked to the ongoing global warming. In summary, during MHW periods, the equatorial central Pacific plays a crucial regulatory role in the interannual anomalies of global pCO2sea; whereas during MCW periods, it may dominate the interannual anomalies of global FCO2 across oceanic regions.

Furthermore, we conducted a detailed analysis of the globally significant positive anomalies in FCO_2 during the 2000 Marine Cold Wave (MCW) period (Figure 1g). The results, illustrated in Figure 5e, reveal notable increases in FCO2 anomalies in the subpolar North Pacific, the equatorial central Pacific, and the subpolar Southern Ocean. Such a pattern is relatively rare in other years characterized by non-significant positive FCO_2 anomalies associated with different MCWs. Similarly, during the 1997 Marine Heat Wave (MHW), we observed significant negative anomalies in pCO_{2sea} (Figure 3g), with the equatorial central Pacific exhibiting a marked decrease in

pCO2sea (Figure 4f). This characteristic is also infrequent in other years associated with MHWs that did not show significant negative pCO_{2sea} anomalies. The underlying drivers of these significant anomaly years warrant further investigation.

4.2、The driving mechanism of pCO_{2sea} change during MHW and MCW in the central Equatorial Pacific Ocean

During the periods of Marine Heat Waves (MHW) and Marine Cold Waves (MCW) in the central Pacific Ocean, the region exhibited a negative contribution to global FCO_2 anomalies. The anomalies in pCO_{2sea} were primarily driven by non-temperature factors, although the key driving processes remain unclear. This study employs least squares linear regression and a random forest model to analyze the impact of various physical factors on FCO2 changes during MHW and MCW events from both linear and nonlinear perspectives, aiming to elucidate the main driving mechanisms.

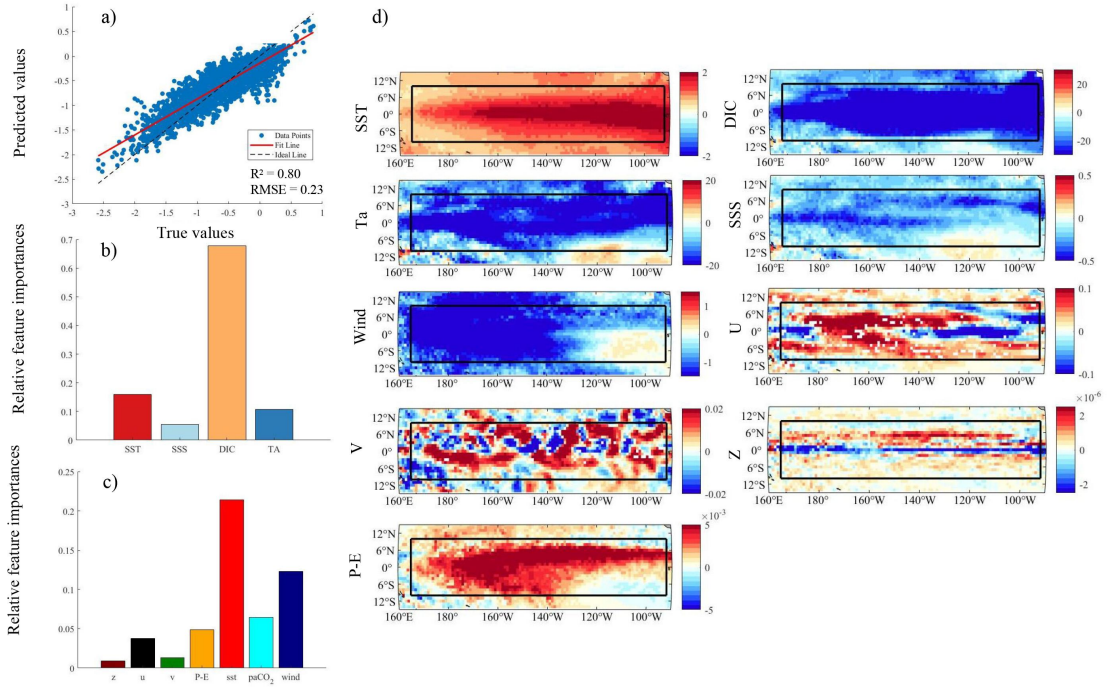

Figure 5. The variation of each element and its significance to the FCO_2 anomalies during equatorial Pacific MHW. Where P-E denotes the freshwater flux resulting from precipitation and evaporation.

During the marine heatwave (MHW) event, the performance of the least squares

regression model was suboptimal (R^2 = 0.42, RMSE = 0.62, $p < 0.05$), while the random forest model demonstrated superior performance (R^2 = 0.80, RMSE= 0.23, $p < 0.05$). The results of the regression analysis indicated that the regression coefficients for vertical flow, lateral flow, radial flow, freshwater flux, sea surface temperature (SST), partial pressure of CO2 (paCO2), and wind speed anomalies were 0.34, -0.29, -0.28, -0.61, -1.79, -0.23, and 1.37, respectively. Feature importance assessment revealed that SST was the primary driver of FCO_2 variability, followed by wind speed.

Further analysis indicated that during the MHW, SST increased by 1.46 ℃, while dissolved inorganic carbon (DIC) and total alkalinity (TA) decreased by 35.98 μmol kg^{-1} and 16.84 μmol kg^{-1}, respectively, with only a minor change in sea surface salinity (SSS) of -0.21 PSU. DIC was found to be the primary non-temperature factor contributing to the reduction in pCO_{2sea} (Figure 5b). Additionally, changes in wind speed during the MHW exhibited regional variability: wind speeds decreased on the western side while increasing on the eastern side, leading to a decline in FCO_2 on the west and an increase on the east. Overall, vertical flow intensified, facilitating the upwelling of deeper cold waters enriched in DIC and TA, with a noted weakening of vertical flow near the equator and strengthening on the northern and southern flanks. Furthermore, both lateral and radial flows also underwent changes, further modulating air-sea exchange rates and the distribution of surface DIC. The overall increase in freshwater flux (+0.29 mm) contributed to reduced concentrations of surface DIC, TA, and SSS. The correlation coefficients between freshwater flux and DIC, TA, and SSS were r = -0.45, r = -0.48, and r = -0.53, respectively, indicating that the observed reductions were primarily influenced by changes in freshwater flux rather than deep water upwelling.

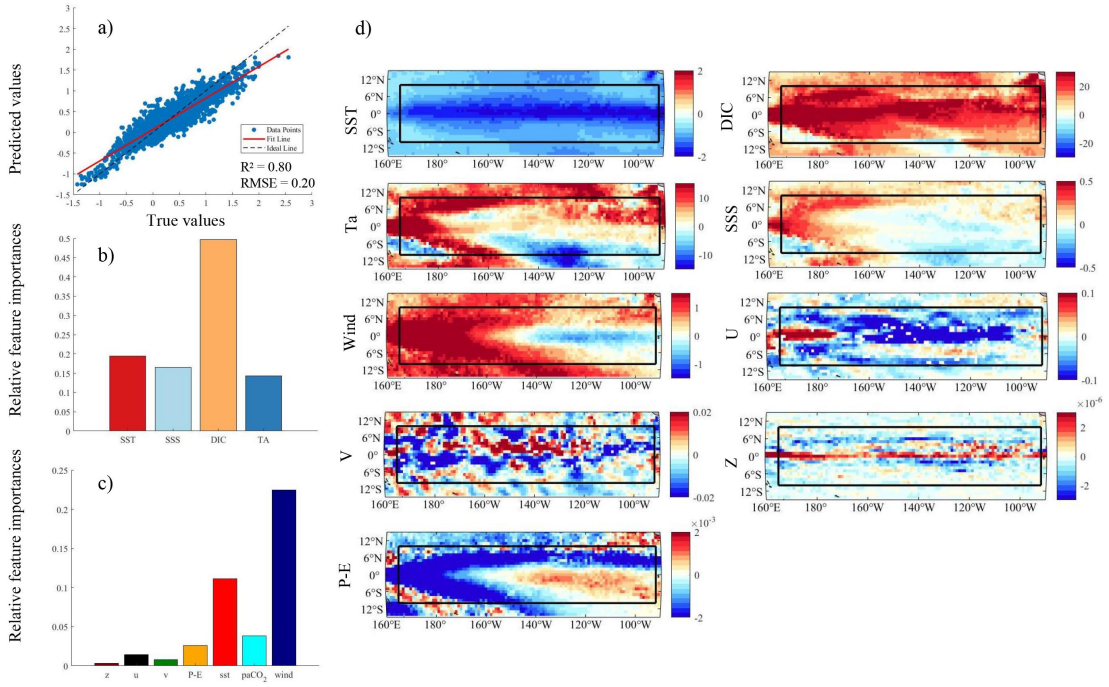

Figure 6. The variation of each element and its significance to the FCO_2 anomalies during equatorial Pacific MCW

During the MCW event, the performance of the least squares regression model was suboptimal (R^2 = 0.47, RMSE = 0.60, $p < 0.05$), whereas the random forest model exhibited superior performance (R^2 = 0.80, RMSE = 0.20, $p < 0.05$). The results of the regression analysis indicated that the regression coefficients for vertical flow, lateral flow, radial flow, freshwater flux, sea surface temperature (SST), partial pressure of CO2 (paCO2), and wind speed anomalies were 0.11, 0.55, -0.13, -0.04, -0.97, -0.32, and 1.17, respectively. Feature contribution analysis revealed that wind speed was the primary driver of FCO2 variability, followed by SST.

During the MCW period, sea surface temperature (SST) decreased by 1.25°C, while dissolved inorganic carbon (DIC) and total alkalinity (TA) increased by 20.72 μmol/kg and 5.04 μmol/kg, respectively. The change in sea surface salinity (SSS) was minimal (+0.06). Among these factors, DIC was identified as the primary non-temperature driver contributing to the increase in pCO_{2sea} (Figure 6b). Wind speed exhibited regional variability, with an intensification on the western side and a reduction on the eastern side, resulting in an increase in FCO2 on the western side and a decrease on the eastern side. Overall, vertical flow decreased, which weakened the

upwelling of deep cold water enriched with DIC and TA; this upwelling was enhanced near the equator while it weakened on the northern and southern flanks. Furthermore, the trends in zonal and meridional flows were opposite to those observed during marine heatwave (MHW) events, suggesting that they may have played a significant role in the changes in FCO2 by altering horizontal transport processes. The overall freshwater flux decreased by 0.11 mm; however, some areas on the eastern side showed an increasing trend, which further modulated the concentrations of DIC, TA, and SSS. The correlation coefficients between freshwater flux and DIC, TA, and SSS were r = -0.28, r = -0.32, and r = -0.38, respectively, indicating that the overall increase in DIC, TA, and SSS is more likely attributable to changes in freshwater flux rather than deep water upwelling.

During the marine heatwave (MHW) and marine cold wave (MCW) events, the role of vertical flow in influencing FCO2 variations in the equatorial central Pacific is relatively minor. This may be attributed to opposing trends in vertical flow both at the equator and its northern and southern flanks, which weaken the overall impact. During the MHW, the vertical flow near the equator weakened, inhibiting the upwelling of deep waters rich in dissolved inorganic carbon (DIC) and total alkalinity (TA). In contrast, during the MCW, the intensified vertical flow facilitated the upwelling of deep waters. Therefore, in addition to key factors such as wind speed, sea surface temperature (SST), and freshwater flux, the vertical transport processes of equatorial deep water may also play a significant role in influencing FCO2 variations in this region.

5、Conclusion

This study systematically analyzes the spatiotemporal differences in the impacts of Marine Heat Waves (MHWs) and Marine Cold Waves (MCWs) on the flux of carbon dioxide (FCO2) and their underlying physical mechanisms. The results indicate that between 1990 and 2019, the influence of extreme temperature events on global oceanic FCO2 transitioned from being predominantly driven by MCWs to

being primarily influenced by MHWs. Both phenomena exert significant yet opposing effects on global oceanic FCO2 regulation: MHWs are associated with a reduction in global ocean CO2 absorption by approximately 0.112 PgC, while MCWs contribute to an increase of about 0.312 PgC, with the impact intensity of MCWs being roughly three times that of MHWs. Notably, the trends in FCO2 in the subpolar North Pacific, Arabian Sea, equatorial central Pacific, and subpolar Southern Ocean exhibit distinct regional responses that contrast with the global trend. Further mechanistic analysis reveals significant differences in the dominant controlling factors of FCO2 changes across different oceanic regions: in the Arabian Sea, FCO2 variations are primarily regulated by wind speed, whereas in the subpolar North Pacific, equatorial central Pacific, and subpolar Southern Ocean, changes in pCO2sea are the main driving force.

During marine heatwave (MHW) and marine cold wave (MCW) events, although the changes in sea surface pCO2 (pCO2sea) in most oceanic regions are primarily regulated by temperature, notable influences from non-temperature factors are observed in the subpolar North Pacific, the equatorial central Pacific, and the subpolar Southern Ocean. In particular, the non-temperature regulatory effects in the equatorial central Pacific are especially pronounced, and this region plays a significant role in the interannual responses of global oceanic FCO2 and pCO2sea to extreme temperature events. To investigate the driving mechanisms behind the changes in pCO2sea in this region, we employed linear regression and random forest models to systematically assess the relative contributions of various factors to FCO2 and pCO2sea during MHW and MCW periods. The results indicate that during MHW, sea surface temperature (SST) is the primary driver of FCO2 changes, followed by wind speed. Conversely, during MCW, wind speed becomes the main driver of FCO2 changes, with SST following. Throughout both MHW and MCW periods, dissolved inorganic carbon (DIC) emerges as the principal non-temperature factor contributing to the rise in pCO2sea. The underlying mechanisms involve freshwater fluxes, which modulate the concentrations of DIC, total alkalinity (TA), and sea surface salinity (SSS), thereby directly affecting the equilibrium of the seawater carbonate system.

Additionally, vertical flow in the equatorial region influences the upwelling intensity of deep waters with high DIC and TA, indirectly regulating surface pCO2sea. Furthermore, both zonal and meridional currents can affect FCO2 changes by altering horizontal transport processes. These findings enhance our understanding of the regulatory mechanisms of the oceanic carbon cycle during extreme temperature events and provide a scientific basis for accurately assessing changes in oceanic carbon sinks.

Future research directions should focus on the following aspects: (1) A comprehensive investigation into the combined effects of extreme temperature events and other extreme events on oceanic carbon flux, particularly the long-term impacts of recurrent compound extreme events on regional and global carbon cycling; (2) The development of a more accurate assessment framework for the coupling of extreme events and carbon cycling, utilizing high-resolution ocean circulation models, biogeochemical models, and multi-source satellite observation data. With advancements in observational technologies and improvements in model resolution, our understanding of the interactions between extreme ocean events and the carbon cycle will continue to deepen, providing a robust scientific basis for the precise assessment of oceanic carbon sinks in the context of global climate change.

Conflict of Interest

The authors declare that they have no conflict of interests.

Reference

Alizadeh O. A review of ENSO teleconnections at present and under future global warming[J]. Wiley Interdisciplinary Reviews: Climate Change, 2024, 15(1): e861.

Athira K S, Attada R, Rao V B. Synoptic dynamics of cold waves over north India: Underlying mechanisms of distinct cold wave conditions[J]. Weather and Climate Extremes, 2024, 43: 100641.

Boer G J. The ratio of land to ocean temperature change under global warming[J]. Climate dynamics, 2011, 37(11): 2253-2270.

Collins M, An S I, Cai W, et al. The impact of global warming on the tropical Pacific Ocean and El Niño[J]. Nature Geoscience, 2010, 3(6): 391-397.

Chiswell S M. Global trends in marine heatwaves and cold spells: the impacts of fixed versus changing baselines[J]. Journal of Geophysical Research: Oceans, 2022, 127(10): e2022JC018757.

Deser C, Phillips A S, Alexander M A, et al. Future changes in the intensity and duration of marine heat and cold waves: insights from coupled model initial-condition large ensembles[J]. Journal of Climate, 2024, 37(6): 1877-1902.

DeVries T, Le Quéré C, Andrews O, et al. Decadal trends in the ocean carbon sink[J]. Proceedings of the National Academy of Sciences, 2019, 116(24): 11646-11651.

DeVries T, Yamamoto K, Wanninkhof R, et al. Magnitude, trends, and variability of the global ocean carbon sink from 1985 to 2018[J]. Global Biogeochemical Cycles, 2023, 37(10): e2023GB007780.

Duke P J, Hamme R C, Ianson D, et al. Estimating marine carbon uptake in the northeast Pacific using a neural network approach[J]. Biogeosciences, 2023, 20(18): 3919-3941.

Edwing K, Wu Z, Lu W, et al. Impact of marine heatwaves on air-sea CO2 flux along the US east coast[J]. Geophysical Research Letters, 2024, 51(1): e2023GL105363.

Fay A R, Munro D R, McKinley G A, et al. Updated climatological mean Δ f CO2 and net sea–air CO2 flux over the global open ocean regions[J]. Earth System Science Data, 2024, 16(4): 2123-2139.

Friedlingstein P, O'Sullivan M, Jones M W, et al. Global carbon budget 2024[J]. Earth System Science Data Discussions, 2024, 2024: 1-133.

Frölicher T L, Fischer E M, Gruber N. Marine heatwaves under global warming[J]. Nature, 2018, 560(7718): 360-364.

Frölicher T L, Laufkötter C. Emerging risks from marine heat waves[J]. Nature communications, 2018, 9(1): 650.

Guo X, Gao Y, Zhang S, et al. Threat by marine heatwaves to adaptive large marine ecosystems in an eddy-resolving model[J]. Nature climate change, 2022, 12(2): 179-186.

Holbrook N J, Scannell H A, Sen Gupta A, et al. A global assessment of marine heatwaves and their drivers[J]. Nature communications, 2019, 10(1): 2624.

Iida Y, Kojima A, Takatani Y, et al. Trends in pCO2 and sea–air CO2 flux over the global open oceans for the last two decades[J]. Journal of Oceanography, 2015, 71: 637-661.

Laufkötter C, Zscheischler J, Frölicher T L. High-impact marine heatwaves attributable to human-induced global warming[J]. Science, 2020, 369(6511): 1621-1625.

Li C, Burger F A, Raible C C, et al. Observed regional impacts of marine heatwaves on sea-air CO2 exchange[J]. Geophysical Research Letters, 2024, 51(24): e2024GL110379.

Mandal R, Joseph S, Sahai A K, et al. Diagnostics and real-time extended range prediction of cold waves over India[J]. Climate Dynamics, 2023, 61(5): 2051-2069.

Meque A O, Pinto I S, Chuwah C. Spatial variability of cold waves over Southern Africa and their potential physical mechanisms[J]. Environmental Research: Climate, 2024, 3(4): 045029.

Mignot A, Von Schuckmann K, Landschützer P, et al. Decrease in air-sea CO2 fluxes caused by persistent marine heatwaves[J]. Nature Communications, 2022, 13(1): 4300.

Oliver E C J, Donat M G, Burrows M T, et al. Longer and more frequent marine heatwaves over the past century[J]. Nature communications, 2018, 9(1): 1324.

Quesada B, Vautard R, Yiou P. Cold waves still matter: characteristics and associated climatic signals in Europe[J]. Climatic Change, 2023, 176(6): 70.

Ratnam J V, Behera S K, Annamalai H, et al. ENSO's far reaching connection to Indian cold waves[J]. Scientific reports, 2016, 6(1): 37657.

Resplandy L, Hogikyan A, Müller J D, et al. A synthesis of global coastal ocean

greenhouse gas fluxes[J]. Global Biogeochemical Cycles, 2024, 38(1): e2023GB007803.

Sarma V, Sridevi B, Metzl N, et al. Air-Sea fluxes of CO2 in the Indian Ocean between 1985 and 2018: A synthesis based on Observation-based surface CO2, hindcast and atmospheric inversion models[J]. Global Biogeochemical Cycles, 2023, 37(5): e2023GB007694.

Smith K E, Burrows M T, Hobday A J, et al. Socioeconomic impacts of marine heatwaves: Global issues and opportunities[J]. Science, 2021, 374(6566): eabj3593.

Yao Y, Wang C, Fu Y. Global marine heatwaves and cold-spells in present climate to future projections[J]. Earth's Future, 2022, 10(11): e2022EF002787.

Yang X, Wynn-Edwards C A, Strutton P G, et al. Drivers of air-sea CO2 flux in the subantarctic zone revealed by time series observations[J]. Global Biogeochemical Cycles, 2024, 38(1): e2023GB007766.